MOLECULAR IMAGING AND BIOLOGY

World Molecular Imaging Society

RESEARCH ARTICLE

GRP Receptor Imaging of Prostate Cancer Using [99mTc]Demobesin 4: a First-in-Man Study

Stephen J. Mather,[1] Berthold A. Nock,[2] Theodosia Maina,[2] Vickie Gibson,[3]
David Ellison,[1] Iain Murray,[3] Ravin Sobnack,[3] Steve Colebrook,[4] Susan Wan,[4]
Gavin Halberrt,[5] Teresa Szysko,[1,5] Thomas Powles,[1] Norbert Avril[1,5]

[1]Centre for Molecular Oncology, Barts Cancer Institute, London, EC1M 6BQ, UK
[2]Molecular Radiopharmacy, INRASTES, NCSR "Demokritos", 15310, Athens, Greece
[3]Department Nuclear Medicine, St Bartholomews Hospital, Barts NHS Trust, London, EC1A 7BE, UK
[4]Drug Development Office, Cancer Research UK, London, EC1V4AD, UK
[5]Cancer Research UK Formulation Unit, Strathclyde Institute of Pharmacy and Biomedical Sciences, University of Strathclyde, Glasgow, G4 0RE, UK

Abstract

Purpose: We explored the imaging of bombesin receptors and evaluated the clinical use of [99mTc]Demobesin 4 ([99mTc]DB4) in prostate cancer patients.
Procedures: [99mTc]DB4 was prepared according to Good Manufacturing Practice. Patients with prostate cancer underwent serial planar and SPECT imaging up to 3 h after administration. Blood and urine samples were taken to assess pharmacokinetics.
Results: [99mTc]DB4 is safe and clears rapidly from the bloodstream via the kidneys resulting in low background activity. The tracer binds strongly to the gastrin-releasing peptide receptor (GRPR) *in vivo* as indicated by the high uptake in the pancreas seen in all patients. In patients who had undergone hormone therapy, [99mTc]DB4 did not efficiently image metastatic prostate cancer. In contrast, in newly diagnosed patients local disease was visualised.
Conclusions: The GRPR is an unsuitable target for imaging refractory prostate cancer but may be useful in untreated disease. [99mTc]DB4 is a promising radiopharmaceutical which merits further exploration in this specific group of patients.

Key words: GRP receptor, Peptide, Imaging, Tc-99m

Introduction

There is a strong need to develop appropriate imaging agents for prostate cancer [1, 2]. Prostate cancer has a better

Correspondence to: Stephen Mather; *e-mail:* s.j.mather@qmul.ac.uk

chance of successful treatment if detected early, when it is still confined to the prostate gland. However, the diagnosis of primary tumours within the prostate gland often requires multiple biopsies and imaging could guide such biopsies and ideally reduce the number of unnecessary biopsies. Currently, ultrasound (US) and magnetic resonance imaging (MRI) are the two main imaging methods used for detection of prostate cancer [3]. However, transrectal ultrasound is limited by poor tissue resolution, and although the soft tissue contrast is better for MRI, it is expensive and often not able to identify and characterise early prostate cancer. In addition, the detection of distant metastases relies

on bone scintigraphy for identification of skeletal metastases and on CT for both bone and soft tissue metastases [2].

Using radiolabelled receptor ligands has been highly successful for imaging the expression of somatostatin receptors for conventional gamma camera imaging and positron emission tomography [4]. We explored the exploitation of bombesin receptor imaging with Tc-99m and evaluated the potential clinical use in prostate cancer patients.

Bombesin (BN) is a peptide of amphibian origin, but the human counterpart gastrin-releasing peptide (GRP) shows considerable similarity in structure, especially in the seven C-terminal residues which are identical. GRP (and BN) binds to the gastrin-releasing peptide receptor (GRPR) which has been widely reported to be overexpressed in a number of tumour types notably prostate and breast, but also small cell lung cancer, renal cell carcinoma and gastrointestinal stromal tumours (GIST) [5–10]. The first *in vitro* study to explore the targeting of radiolabelled bombesin analogues in cancer was published in 1995 [11], and this was followed by numerous papers describing the pre-clinical development of many BN analogues labelled with a variety of radionuclides.

The first clinical use of a BN-based radiopharmaceutical, performed by van der Wiele in 2000 using [^{99m}Tc]RP527 [^{99m}Tc]-N$_3$S-Gly-5-Ava-BN [7–14], showed some promise with tumour uptake seen in four of six breast cancers and one of four androgen-resistant bone-metastasized prostate carcinomas [12]. Since that time, however, very few clinical evaluations of BN analogues have been reported. Three peer-reviewed papers were published by Scopinaro et al. who in 2002–2004 described the use of another technetium-labelled analogue [^{99m}Tc] [Leu^{13}]BN for imaging breast, prostate and colorectal cancer in which promising results were seen in all indications [13–15]. Some further clinical studies have been performed but published only in abstract form [16–20].

This relative dearth of objective clinical evaluations of radiolabelled bombesin-based radiopharmaceuticals has been highlighted by reviewers who have called for further clinical trials to be performed, especially in prostate cancer [21].

Despite the clear logistical and economical attractions of a technetium-99m-labelled radiopharmaceutical, one of the shortcomings of many of these compounds is their relatively high lipophilicity resulting in significant hepatobiliary excretion leading to a consequent difficulty in identifying tumours in the abdomen [22]. A successful strategy for decreasing the lipophilicity of radiolabelled peptides has been the use of the hydrophilic tetraamine ([^{99m}Tc](O$_2$)-N$_4$)chelator system [23]. Using this approach, Nock et al. developed a series of hydrophilic technetium-labelled bombesin-based agonists and antagonists which showed promise for imaging GRPR expressing tumours in animal models [24].

This paper describes the evaluation of one of this series, [^{99m}Tc]Demobesin 4 ([^{99m}Tc]DB4), in a small group of patients with prostate cancer.

Methods

The trial was undertaken under the sponsorship and management of Cancer Research UK's Drug Development Office.

[^{99m}Tc]DB4 Preparation

The radiolabelled DB4 was manufactured in strict accordance with European Union (EU) Good Manufacturing Practice (GMP) [25] following the methodology described by Nock et al. [7] and Decristoforo et al. [26]. Clinical-grade DB4 (N4-Pro-Gln-Arg-Tyr-Gly-Asn-Gln-Trp-Ala-Val-Gly-His-Leu-Nle-NH$_2$ peptide conjugate, N4 = 6-(p-carboxyl)-1,4,8,11-tetraazaundecane), was synthesised by Pichem (Graz, Austria), and all other chemicals were purchased in Pharmacopoeial grade. The reagents required were formulated into sterile single-use products by the Cancer Research UK Formulation Unit, Strathclyde Institute of Pharmacy and Biomedical Sciences. DB4 peptide was stored at −20 °C and buffers between 15 to 25 °C. Five hundred microlitres (1,000 MBq) of sodium [^{99m}Tc]pertechnetate eluted from a ^{99}Mo/^{99m}Tc generator (GE Healthcare) was added to 100 µl 0.25 M phosphate buffer solution pH 11.5 and 5 µl 0.1 M tri-sodium citrate buffer followed by 5.5 µl (5.5 nmol, 10 µg) DB4 peptide 1 mM in 0.1 % acetic acid/ethanol 80:20. Twenty microlitres (60 µg) of a freshly prepared solution of stannous chloride dihydrate in absolute ethanol was then added and the mixture incubated at room temperature for 30 min. The preparation was finally diluted to 5 ml with phosphate buffered saline and filtered through a 0.22-µm filter into the final container ready for administration. Each radiolabelled batch of DB4 was assayed for quality control purposes by ITLC and HPLC to confirm radiochemical purity >90 % and radiochemical identity prior to qualified person (QP) release for patient administration in accordance with the approved IMP manufacturing process. An example of an HPLC radiochromatogram is presented in Supplementary Fig. 1S. Sterility was confirmed by retrospective sterility tests following radioactive decay of the product.

Patient Selection

This was a single-centre, non-therapeutic phase I trial of [^{99m}Tc]DB4 for imaging prostate cancer. Eligible patients were ≥18 years, had histologically proven prostate cancer from biopsy samples and a World Health Organisation (WHO) performance status of 0, 1 or 2. For the purpose of the study, the patients were stratified into two groups:

Group 1—patients with cancer confined to the prostate (proceeding to radical prostatectomy post-imaging);
Group 2—patients with metastatic disease.

Adequate bone marrow, renal and hepatic function was required (haemoglobin≥9.0 g/dl; neutrophils≥1.5×10^9/L; platelets≥100×10^9/L; serum bilirubin≤1.5× upper limit of normal; serum creatinine≤1.5× upper limit of normal), and these were evaluated within 1 week prior to the patient starting the trial.

Patients undergoing chemotherapy or radiotherapy during the 2 weeks prior to study or scheduled within 2 weeks post-study were

excluded, as well as those with partners of child-bearing potential unless they agreed to take measures not to father children during the trial and for 6 months afterwards. Further exclusion criteria included major thoracic and/or abdominal surgery, active uncontrolled infection, cardiac arrhythmia and significant cardiac disease.

Baseline staging of the patient's prostate cancer was performed by CT or MRI and [^{99m}Tc]MDP bone scan within 4 weeks of the [^{99m}Tc]DB4 administration. A full history, physical examination, electrocardiograms (ECGs) and urinalysis were undertaken in the week prior to the [^{99m}Tc]DB4 administration. Informed consent for the study was obtained.

[^{99m}Tc]DB4 Administration

A single 5-ml dose of 500–800 MBq [^{99m}Tc]DB4 (equivalent to 8 to 12 μg DB4 peptide) was administered as a slow IV injection over 1 min. No premedication was required prior to injection with [^{99m}Tc]DB4.

Safety

Vital signs (pulse rate, systolic and diastolic BP) were measured prior to the injection of [^{99m}Tc]DB4 as well as within 15 min post-injection. Similarly, ECGs were performed prior to the injection, continuously during the injection and for 15 min post-injection. ECG and vital signs were repeated again after the last scan has been performed and also blood tests for haematology and biochemistry.

Adverse events (AEs) were assessed and graded according to National Cancer Institute [27] Common Toxicity Criteria for Adverse Events (CTCAE) Version 3.0. Patients were assessed for toxicity from the time of consent until 28 days after the single administration of [^{99m}Tc]DB4. If any AEs attributed as almost certainly, probably or possibly related to [^{99m}Tc]DB4 were still present at day 28, the patient would be followed up monthly by the investigator until resolution or stabilisation of the AE.

Image Acquisition

Gamma camera imaging was performed on a BRIGHTVIEW XCT dual-headed SPECT/CT scanner and consisted of dynamic planar imaging over the pelvis at 0–10 min after the end of [^{99m}Tc]DB4 administration, with static planar whole body imaging at 15 min, 1 h and 3 h and an additional SPECT/CT image at 1–3 h. Further, whole body imaging was permitted up to 6 h, but this was not required.

Imaging Data Analysis

The [^{99m}Tc]DB4 scans were jointly reviewed on the HERMES (Nuclear Diagnostics) workstation by two experienced Nuclear Medicine physicians and one senior physicist. Two separate analyses were undertaken, namely tracer uptake in the prostate gland and tracer uptake in metastatic disease. [^{99m}Tc]DB4 uptake was graded visually as present, equivocal or absent. The scans were then compared to conventional imaging techniques (CT, MR, bone scan) to allow comparison of any abnormal [^{99m}Tc]DB4 uptake with other imaging modalities and conversely allow analysis of

abnormal findings on anatomical imaging with the [^{99m}Tc]DB4 uptake of corresponding lesions.

Pharmacokinetic (PK) Methods

Eleven 3-ml blood samples were collected at the following times on study day 1: pre-dose, 5, 10, 20, 45 min, 1, 2, 3, 4 and 6 h post-dose. Blood samples (2×1 ml aliquots) were weighed and radioactivity counted in a gamma counter together with radioactive standards. The percentage of the injected radioactive dose in the blood at each time point was then calculated and non-linear regression analysis performed to calculate the clearance half-time. All patients were also requested to collect their urine for up to 6 h post-administration of [^{99m}Tc]DB4, and all samples were combined in one 24-h urine collection container. The total volume of urine collected was measured and radioactivity counted (in 2×1 ml aliquots) using a gamma counter together with radioactive standards. The percentage of the injected dose in the urine sample collected was then calculated.

Radiation Dosimetry

Dosimetry was performed using data obtained from conjugate view whole body images. Region of Interest (ROI) analysis was used to measure the number of counts in the pancreas, kidneys and bladder. Counts were corrected for attenuation and converted to measurements of radioactivity using the method of Siegel [17]. Residence times were estimated by integrating the activity time curves up to the time of the last whole body image acquisition and then assuming physical decay only until $t=\infty$. Dosimetry calculations were performed with the OLINDA software (Vanderbilt University) using residence times for the kidneys, pancreas, urinary bladder contents and the remainder of the body as input values.

In addition to the clearance from blood, the kinetics associated with tumour deposits were also investigated when possible. ROIs were placed on the dynamic images as well as on whole body images. Background activity was corrected using a mirrored contralateral ROI.

Results

Pharmacokinetics

[^{99m}Tc]DB4 followed a bi-exponential clearance from the blood with the majority (approximately 80 %) of the peptide being cleared with a distribution half-life of 3.4 min and the remaining 20 % with a slower elimination half-life of 1.7 h. An example of a blood clearance profile is presented in Supplementary Fig. 2S. The major route of clearance is through the kidney with most patients excreting more than 50 % of the peptide within 6 h of administration. Little gastrointestinal excretion was observed resulting in very low non-specific accumulation in the abdomen. The calculated pharmacokinetic parameters are presented in Table 1.

In terms of radiation dosimetry, [^{99m}Tc]DB4 accumulated principally in the pancreas of all subjects. Table 2 shows the

Table 1. Pharmacokinetic parameters for [^{99m}Tc]Demobesin 4

Parameter	Mean	Standard deviation
VD (L)	6.24	±1.63
A1 (%)	78.31	±6.69
k1 (h^{-1})	12.18	±2.83
A2 (%)	21.69	±6.69
k2 (h^{-1})	0.40	±0.08

radiation dosimetry across all organs. For an administration of 600 MBq, the highest absorbed doses were 23.7, 21.1 and 9.4 mGy to the pancreas, urinary bladder wall and kidneys, respectively. For the same administered activity, the effective dose was 3.1 mSv.

Safety

All patients showed a transient increase in heart rate, which normalised within minutes after tracer injection. In the eight patients studied, a total of 14 AEs were recorded, but all of these were considered to be unrelated to [^{99m}Tc]DB4 administration. No AEs met the protocol defined criteria of a dose limiting toxicity. The most common events were gastrointestinal AEs, which were reported in three patients and included nausea, vomiting, diarrhoea, constipation and dysgeusia with CTCAE grades ranging from 1 to 3 and pain, with four patient cases, three of which were specifically reported as bone pain with maximum CTCAE grades 2 or 3. Of the four patient reports, all events were considered to be unrelated to [^{99m}Tc]DB4 administration, with three of the patients having a pre-existing medical history record of pain.

Table 2. Radiation dosimetry of [^{99m}Tc]Demobesin 4

Organ	Absorbed dose/mGy/MBq	Standard deviation
Adrenals	3.87×10^{-3}	9.41×10^{-4}
Brain	1.49×10^{-3}	5.35×10^{-4}
Breasts	1.31×10^{-3}	4.45×10^{-4}
Gallbladder wall	3.47×10^{-3}	9.01×10^{-4}
LLI wall	3.94×10^{-3}	1.45×10^{-3}
Small intestine	3.19×10^{-3}	9.66×10^{-4}
Stomach wall	3.50×10^{-3}	8.87×10^{-4}
ULI wall	2.96×10^{-3}	8.80×10^{-4}
Heart wall	2.41×10^{-3}	7.30×10^{-4}
Kidneys	1.56×10^{-2}	4.95×10^{-3}
Liver	2.61×10^{-3}	7.25×10^{-4}
Lungs	1.97×10^{-3}	6.28×10^{-4}
Muscle	2.21×10^{-3}	6.73×10^{-4}
Ovaries	3.94×10^{-3}	1.41×10^{-3}
Pancreas	3.95×10^{-2}	1.23×10^{-2}
Red marrow	2.19×10^{-3}	6.46×10^{-4}
Osteogenic cells	5.40×10^{-3}	1.75×10^{-3}
Skin	1.30×10^{-3}	4.17×10^{-4}
Spleen	3.83×10^{-3}	9.27×10^{-4}
Testes	2.69×10^{-3}	9.77×10^{-4}
Thymus	1.83×10^{-3}	6.31×10^{-4}
Thyroid	1.79×10^{-3}	6.42×10^{-4}
Urinary bladder wall	3.52×10^{-2}	2.21×10^{-2}
Uterus	6.04×10^{-3}	2.70×10^{-3}
Effective dose/mSv/MBq	5.19×10^{-3}	1.7×10^{-3}

Imaging

Eight patients received [^{99m}Tc]DB4 as a single administration at a dose of 500–800 MBq (equivalent to 8 to 12 µg DB4 peptide) by slow IV injection over 1 min. Two were from group 1 (initial diagnosis of prostate cancer with no treatment) and six from group 2 (known metastatic disease—all of whom had previous hormone treatment). Median age was 65.5 years (range 56–77 years). There was no cumulative exposure as each patient received only one administration of [^{99m}Tc]DB4 (Table 3).

The [^{99m}Tc]DB4 planar and SPECT/CT imaging was visually evaluated for increased uptake in the primary tumour and sites of metastatic disease (bone, lymph nodes and other) and compared to conventional imaging (bone scan and CT) and, where available, MRI. The results are summarised in Table 4.

Dynamic gamma camera imaging revealed increased activity in the large pelvic vessels, which disappeared at approximately 6–10 min after tracer injection (on the anterior views). Bladder activity was first visualised at approximately 4–6 min. In patients 5 and 6, the increased activity in the large pelvic vessels did not disappear during imaging (up to 3 h after injection) and there was poor renal tracer clearance. Nevertheless, bladder activity was visualised at approximately 6 min.

On delayed whole body imaging, there was intensely increased tracer binding in the pancreas in all patients as the gastrin-releasing peptide receptor (GRPR) is highly expressed in the pancreas in humans (Figs. 1 and 2). Mildly increased [^{99m}Tc]DB4 activity was noted in the gastrointestinal (GI) tract. In patient 6, the tracer excretion into the bowel increased over time and there was significant gut activity noticed at 3 h after injection.

Focal uptake in the prostate gland, corresponding to the site of the primary tumour on MR, was seen in both the dynamic and static imaging in the two patients from group 1 (patients 7 and 8) who had received no prior treatment Uptake was greater at 1 h than at 15 min and best visualised on the SPECT/CT imaging (Fig. 3). There was no [^{99m}Tc]DB4 uptake in the prostate gland in the six patients who had received previous hormone treatment (patients 1–6).

There was no evidence for increased [^{99m}Tc]DB4 binding in pelvic lymph nodes in either group 1 or group 2 patients and no additional [^{99m}Tc]DB4 avid metastatic lesions identified in the group 1 patients, who, by definition had early-stage disease on MR.

Table 3. Patient demographics

Number of patients administered [^{99m}Tc]DB4	8
Median age in years (range)	65.5 (56 to 77)
Number of patients in each patient group	
Group 1	2
Group 2	6
Number of patients found to be ineligible/not administered [^{99m}Tc]DB4	2

Table 4. Comparison of [^{99m}Tc]DB4 planar and SPECT/CT imaging to conventional imaging (bone scan and CT) and MRI

Patient no	Age (years)	Group	PSA	Prior hormone therapy?	[^{99m}Tc]DB4 imaging results					Other imaging results
					Prostate	LN	Bone	Other	Summary	
1	60	2	52	Y	−	−	5th rib-; spine T12-RIPR ++	−	One bone lesion ++	Extensive bone disease
2	68	2	150	Y	−	−	−	−	−	Extensive bone disease
3	77	2	43	Y	−	−	Spine L5 ++ R femur ++ L iliac crest ++	−	Few bone lesions	Extensive bone disease
4	74	2	20	Y	−	−	−	−	−	Extensive bone disease
5	74	2	88	Y	−	−	−	−	−	Extensive bone disease
6	56	2	2.3	Y	−	−	6th rib ++	Liver met ++	Liver and bone mets ++	Liver mets and extensive bone disease
7	63	1	7.4	N	++	−	−	−	SPECT shows primary ++	MRI shows primary tumour
8	58	1	4.3	N	++	−	−	−	SPECT shows primary ++	MRI shows primary tumour

*LN* lymph nodes, *RIPR* right inferior pubic ramus

Variable [^{99m}Tc]DB4 uptake was demonstrated in skeletal metastases. In half of the patients with metastatic disease to the bone, the lesions were not visualised at all using [^{99m}Tc]DB4 imaging. Patient 2 had extensive bone metastatic disease in the central skeleton on CT and bone scan, as well as nodal disease, but there was no [^{99m}Tc]DB4 uptake at these sites. Patient 4 had pelvic nodal disease and a suspicious lesion in a left rib, but no [^{99m}Tc]DB4 uptake at these sites. Patient 5 had extensive bone metastatic disease in the central skeleton on CT and bone scan, but not visualised by [^{99m}Tc]DB4.

Three of the six patients from group 2, however, did demonstrate increased [^{99m}Tc]DB4 binding in some bone

Fig. 1 Bone scan of patient 3 with advanced stage of prostate cancer showing multiple bone metastases (*black areas*) throughout the skeleton (see *arrows*).
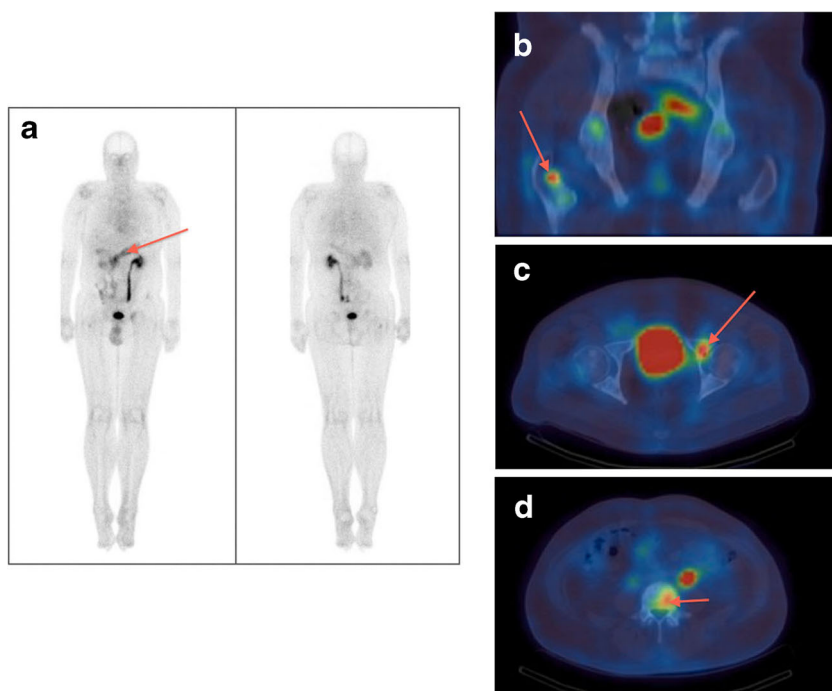
Fig. 2 [^{99m}Tc]DB4 imaging of Patient 3. **a** Whole body planar imaging at 1 h after injection shows increased uptake in the pancreas (*arrowed*) and low tracer excretion into the bowel but little uptake in bone lesions. **b** Spot views from SPECT/CT demonstrate increased [^{99m}Tc]DB4 uptake in the right proximal femur, **c** the left anterior pubic ramus and **d** in the lower lumbar spine.

lesions. Patient 1 had uptake in a right inferior pubic ramus lesion on both the dynamic and static lesion (best seen on SPEC/CT at 90 min). This lesion was also seen on CT and demonstrated uptake on bone scan. However, conventional imaging also revealed a lesion in the T12 vertebral body, which did not show [^{99m}Tc]DB4 uptake and also a small lesion seen in the left 5th rib on bone scan, which was also negative on [^{99m}Tc]DB4 uptake. Patient 3 had extensive bone metastatic disease in the central and axial skeleton on CT and bone scan (Fig. 1). Increased [^{99m}Tc]DB4 binding was demonstrated in lesions in the L5 vertebral body, the right proximal femur and in the left iliac crest (Fig. 2). It appeared that positive [^{99m}Tc]DB4 binding was associated with less sclerotic lesions. SPECT/CT at 90 min after tracer injection did show further foci of increased [^{99m}Tc]DB4 binding in metastatic deposits, but the majority of the extensive bone metastatic disease was not visualised. Positive foci on [^{99m}Tc]DB4 appeared to have progressed more on follow up bone scans than the negative lesions. In summary, extensive metastatic bone disease showed increased [^{99m}Tc]DB4 binding in only a few lesions. Patient 6 demonstrated bone metastases in the pelvis, sacrum, spine, ribs and in the left proximal femur on CT and bone scan. Focally increased [^{99m}Tc]DB4 binding was identified in only a left 6th rib lesion; otherwise, all other known bone metastases were negative. This patient also had multiple liver metastases which had decreased in size following previous therapy, with residual lesions seen on CT particularly in the left lobe of the liver. SPECT/CT showed increased [^{99m}Tc]DB4 binding in a liver metastasis in the

left lobe of the liver. On CT, there was a small metastatic nodule in the lung. Follow-up CT showed progression of liver and lung lesions.

Discussion

This manuscript describes a first-in-man phase 1 clinical trial of the radiotracer [^{99m}Tc]DB4 in patients with prostate cancer. The results show that [^{99m}Tc]DB4 was well tolerated by these eight subjects and following administration cleared rapidly from the bloodstream via the kidneys resulting in low background activity. The tracer binds strongly to the gastrin-releasing peptide receptor (GRPR) *in vivo* as indicated by the high uptake in the pancreas seen in all patients. The presence of GRPR in the normal human pancreas was previously highlighted through imaging by Froberg [28] and confirmed by histology [29]. Owing to logistic and local regulatory difficulties, only eight patients could be recruited to the study, and although the intention was to investigate patients with cancers ranging from newly diagnosed to late stage, in practice the majority of patients recruited had metastatic disease and had undergone extensive prior therapy (group 2). Only two patients from group 1 with newly diagnosed cancer confined to the prostate and no patients from with locally advanced disease were recruited.

[^{99m}Tc]DB4 did not efficiently image metastatic disease in group 2 patients. There was no increased uptake in the prostate bed or in nodal disease. Uptake in skeletal metastases was variable. Bone lesions demonstrating [^{99m}Tc]DB4 uptake appeared to be less sclerotic, but also
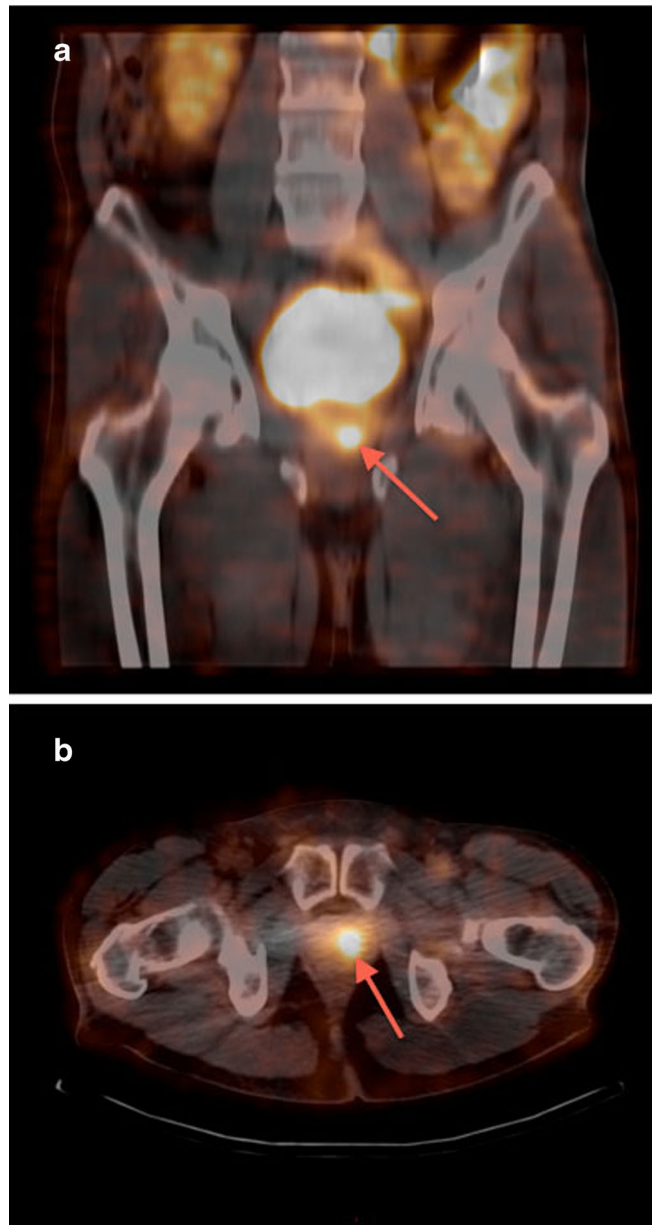
Fig. 3 Patient with newly diagnosed prostate cancer (patient 7). SPECT/CT in **a** coronal and **b** transverse images shows intensely increased [99mTc]DB4 uptake left paramedian in the prostate gland (*arrowed*). This lesion was confirmed histopathologically as prostate cancer.

progressed more than negative lesions on follow-up bone scan. It is important to note that all patients had undergone hormone treatment in Group 2. However, in two patients, [99mTc]DB4 did effectively image newly diagnosed cancer confined to the prostate. Neither of these patients had received any specific therapy for prostate cancer.

Two further papers describing clinical trials of bombesin analogues have been recently published: Kahkonen reported the successful use of the 68Ga-labelled bombesin analogue BAY86-7548 in prostate cancer [27], while in a study by Ananias et al., a further [99mTc]labelled bombesin analogue failed to visualise prostate cancer owing to poor *in vivo* stability of the tracer [30].

The results of the study by Kahkonen which recruited 11 patients with early-stage disease (scheduled for radical prostatectomy) and three patients with post-treatment recurrence [27] are in line with our own. Local disease was successfully imaged in all of the early-stage patients but was less effective in the patients with later-stage disease. These results reflect those obtained in a recent extensive immuno-histochemical analysis of GRPR expression in tissues from 530 patients with prostate cancer [31]. This showed higher receptor expression in early-stage disease and reduced expression in patients with increasing Gleason score, PSA value and tumour size. Pre-clinical imaging studies have shown that GRPR expression is lost following androgen

ablation treatment [21] and a clear correlation exists between GRPR expression and androgen dependence in prostate cancer cell lines [32]. Together, therefore, these two clinical trials indicate that GRPR-binding radiopharmaceuticals are likely to be useful only in early-stage disease prior to androgen ablation and not in the later stages of the disease.

The recent report by Ananias et al. is of an alternative 99mTc-labelled tracer HYNIC(tricine/TPPTS)-Aca-Bombesin [7–14] which failed to image any disease in eight patients with prostate cancer [30]. The reason for this is attributed to the low metabolic stability of this tracer. In contrast, [99mTc]DB4 retained its ability to image receptor expression *in vivo* as evidenced by the high pancreatic uptake. This evidence of high stability *in vivo* is further supported by results of *in vitro* incubation of [99mTc]DB4 in either human (unpublished data) or mouse [24] plasma which also indicate relatively slow metabolism of the tracer in the bloodstream. Further clinical trials of this tracer in patients with early-stage disease to explore its clinical utility are therefore indicated.

Conclusion

The GRPR is an unsuitable target for imaging refractory prostate cancer but may be useful in untreated disease. [99mTc]DB4 is a promising radiopharmaceutical which merits further exploration in this specific group of patients.

Electronic Supplementary Material

Below is the link to the electronic supplementary material.ESM 1(PDF 644 kb)

References

1. Picchio M, Piert M (2013) Prostate cancer imaging. Eur J Nucl Med Mol Imaging 40(Suppl 1):S1–S4
2. Outwater EK, Montilla-Soler JL (2013) Imaging of prostate carcinoma. Cancer Control 20:161–176
3. Murphy G, Haider M, Ghai S, Sreeharsha B (2013) The expanding role of MRI in prostate cancer. AJR Am J Roentgenol 201:1229–1238
4. Geijer H, Breimer LH (2013) Somatostatin receptor PET/CT in neuroendocrine tumours: update on systematic review and meta-analysis. Eur J Nucl Med Mol Imaging 40:1770–1780
5. Gugger M, Reubi JC (1999) Gastrin-releasing peptide receptors in non-neoplastic and neoplastic human breast. Am J Pathol 155:2067–2076
6. Markwalder R, Reubi JC (1999) Gastrin-releasing peptide receptors in the human prostate: relation to neoplastic transformation. Cancer Res 59:1152–1159
7. Nock B, Nikolopoulou A, Chiotellis E et al (2003) [99mTc]Demobesin 1, a novel potent bombesin analogue for GRP receptor-targeted tumour imaging. Eur J Nucl Med Mol Imaging 30:247–258
8. Reubi JC, Korner M, Waser B et al (2004) High expression of peptide receptors as a novel target in gastrointestinal stromal tumours. Eur J Nucl Med Mol Imaging 31:803–810
9. Cornelio DB, Meurer L, Roesler R, Schwartsmann G (2007) Gastrin-releasing peptide receptor expression in cervical cancer. Oncology 73:340–345
10. Jensen RT, Battey JF, Spindel ER, Benya RV (2008) International Union of Pharmacology. LXVIII. Mammalian bombesin receptors: nomenclature, distribution, pharmacology, signaling, and functions in normal and disease states. Pharmacol Rev 60:1–42
11. Hoffman TJ, Sieckman GL, Volkert WA (1995) Targeting small cell lung cancer using iodinated peptide analogs. J Label Compd Radiopharm 37:321–323
12. Van de Wiele C, Dumont F, Vanden Broecke R et al (2000) Technetium-99 m RP527, a GRP analogue for visualisation of GRP receptor-expressing malignancies: a feasibility study. Eur J Nucl Med 27:1694–1699
13. Scopinaro F, De Vincentis G, Corazziari E et al (2004) Detection of colon cancer with 99mTc-labeled bombesin derivative (99mTc -leu13-BN1). Cancer Biother Radiopharm 19:245–252
14. Scopinaro F, De Vincentis G, Varvarigou AD et al (2003) 99mTc -bombesin detects prostate cancer and invasion of pelvic lymph nodes. Eur J Nucl Med Mol Imaging 30:1378–1382
15. Scopinaro F, Varvarigou A, Ussof W et al (2002) Breast cancer takes up 99mTc bombesin. A preliminary report. Tumori 88:S25–S28
16. Bodei L, Ferrari M, Nunn A et al (2007) 177Lu-AMBA bombesin analogue in hormone refractory prostate cancer patients: a phase I escalation study with single-cycle administrations. Eur J Nucl Med Mol Imaging 34:S221
17. Hofmann M, Machens S, Stief C et al (2004) Feasibility of Ga-68-DOTABOM PET in prostate carcinoma patients. Eur J Nucl Med Mol Imaging 31:S253
18. Dimitrakopoulou-Strauss A, Hohenberger P, Haberkorn U et al (2007) 68Ga-labeled bombesin studies in patients with gastrointestinal stromal tumors: comparison with 18F-FDG. J Nucl Med 48:1245–1250
19. Schaefer N, Valencia R, Borkowski S et al (2011) Comparison of BAY 86-4367, a new F-18 labeled bombesin analog, with F-18-ethyl-choline in recurrent and primary prostate cancer patients. J Nucl Med Meet Abstr 52:40
20. Bergsma H, Kulkarni HR, Mueller D et al (2013) PET/CT imaging with a novel 68Ga-labeled GRP-receptor antagonist, sarabesin 3. First clinical data in patients with prostate and breast cancer. J Nucl Med 54:84P
21. Schroeder RP, de Visser M, van Weerden WM et al (2009) Androgen-regulated gastrin-releasing peptide receptor expression in androgen-dependent human prostate tumor xenografts. Int J Cancer 126:2826–2834
22. Van de Wiele C, Dumont F, Dierckx RA et al (2001) Biodistribution and dosimetry of (99 m)Tc-RP527, a gastrin-releasing peptide (GRP) agonist for the visualization of GRP receptor-expressing malignancies. J Nucl Med 42:1722–1727
23. Nock BA, Maina T (2012) Tetraamine-coupled peptides and resulting 99mTc -radioligands: an effective route for receptor-targeted diagnostic imaging of human tumors. Curr Top Med Chem 12:2655–2667
24. Nock BA, Nikolopoulou A, Galanis A et al (2005) Potent bombesin-like peptides for GRP-receptor targeting of tumors with 99mTc: a preclinical study. J Med Chem 48:100–110
25. Commission E (2010) The Rules Governing Medicinal Products in the European Union. Volume 4. EU Guidelines to Good Manufacturing Practice. Annex 13. Investigational Medicinal Products
26. Decristoforo C, Maina T, Nock B et al (2003) 99mTc -demotate 1: first data in tumour patients-results of a pilot/phase I study. Eur J Nucl Med Mol Imaging 30:1211–1219
27. Kahkonen E, Jambor I, Kemppainen J et al (2013) In vivo imaging of prostate cancer using [68Ga]-labeled bombesin analog BAY86-7548. Clin Cancer Res 19:5434–5443
28. Froberg A, Visser M, Maina T et al (2006) Are GRP-receptors present in the human pancreas? J Nucl Med 47:429p
29. Montet X, Yuan H, Weissleder R, Josephson L (2006) Enzyme-based visualization of receptor-ligand binding in tissues. Lab Investig 86:517–525
30. Ananias HJ, Yu Z, Hoving HD et al (2013) Application of 99mTechnetium-HYNIC(tricine/TPPTS)-aca-bombesin(7-14) SPECT/CT in prostate cancer patients: a first-in-man study. Nucl Med Biol 40:933–938
31. Beer M, Montani M, Gerhardt J et al (2012) Profiling gastrin-releasing peptide receptor in prostate tissues: clinical implications and molecular correlates. Prostate 72:318–325
32. de Visser M, van Weerden WM, de Ridder CM et al (2007) Androgen-dependent expression of the gastrin-releasing peptide receptor in human prostate tumor xenografts. J Nucl Med 48:88–93